Monthly Notices
of the
ROYAL ASTRONOMICAL SOCIETY

Mon. Not. R. Astron. Soc. **425,** 1628–1632 (2012) doi:10.1111/j.1365-2966.2012.21498.x

Constraints on sterile neutrino dark matter from *XMM–Newton* observations of M33

E. Borriello,[1,2,3⋆] M. Paolillo,[1] G. Miele,[1,2] G. Longo[1]† and R. Owen[4]

[1]*Università Federico II, Dipartimento di Scienze Fisiche, Via Cintia, I-80126 Napoli, Italy*
[2]*INFN Sezione di Napoli, Via Cintia, I-80126 Napoli, Italy*
[3]*II. Institut für Theoretische Physik, Universität Hamburg, Luruper Chaussee 149, 22761 Hamburg, Germany*
[4]*X-ray & Observational Astronomy Group, Department of Physics & Astronomy, University of Leicester, University Road, Leicester LE1 7RH*

Accepted 2012 June 11. Received 2012 June 11; in original form 2011 October 7

ABSTRACT

Using archival *XMM–Newton* observations of the diffuse and unresolved components' emission in the inner disc of M33, we exclude the possible contribution from narrow line emission in the energy range 0.5–5 keV more intense than 10^{-6}–10^{-5} erg s^{-1}. Under the hypothesis that sterile neutrinos constitute the majority of the dark matter in M33, we use this result in order to put constraints on their parameter space in the 1–10 keV mass range.

Key words: astroparticle physics – line: identification – neutrinos – X-rays: galaxies.

1 INTRODUCTION

One of the main problems of modern astrophysics and cosmology is the unknown nature of the dark matter (DM). Despite the fact that it represents 80 per cent of the matter content of the Universe (Komatsu et al. 2011), it has so far escaped any unambiguous direct detection attempt in underground laboratories. This has given rise to the development of several detection techniques aimed at finding signatures of DM annihilation or decay in the spectrum of cosmic rays (Porter, Johnson & Graham 2011).

On the theoretical side, to solve this puzzle a wide range of possible solutions assuming new physics has been proposed. Standard particles are in fact unable to explain the evidence for the DM, while, e.g., supersymmetric and Kaluza–Klein extension of the standard model are known to provide a rich set of possible DM candidates in terms of weakly interacting massive particles. They have represented the standard assumption about the nature of DM for a long time, and even nowadays they constitute the preferred and most studied candidates in the literature. None the less, many alternative solutions have been proposed. [See Feng (2010), for an up-to-date review.]

Among these, a particularly interesting scenario assumes that DM is instead made up by $\mathcal{O}(1)$ keV sterile neutrinos (Dodelson & Widrow 1994). The well-established discovery of neutrino masses points towards the possible existence of gauge singlet fermions responsible for the neutrino mass generation through a see-saw mechanism. The corresponding masses can range over all known mass scales, but if some of the singlet fermions are light, then sterile neutrinos emerge in the low-energy effective limit of the theory. Such particles are predicted to decay into a lighter neutrino and a photon (Pal & Wolfenstein 1982), producing a narrow line in the X-ray spectrum at an energy equal to half the mass of the decaying neutrino. Such emission is expected to affect the formation of the first stars (Biermann & Kusenko 2006) and to be directly detectable by existing and future X-ray telescopes. Sterile neutrinos could also explain the observed velocities of pulsars, thanks to their anisotropic emission from a cooling neutron star born during the explosion of a supernova. [See Kusenko (2009) for a dedicated review.]

Searches for sterile neutrinos have been conducted in both dwarf and giant galaxies, using all available X-ray observatories. For instance, Loewenstein, Kusenko & Biermann (2009) fail to find signatures of sterile neutrino decay, using the *Suzaku* observations of the Ursa Minor dwarf spheroidal (dSph) galaxy, and placed constraints on the existence of sterile neutrinos with given parameters. However, using the *Chandra* X-ray Observatory, Loewenstein & Kusenko (2010) reported the detection of a narrow emission feature with energy of 2.5 keV in the dSph Willman 1, consistent with emission line from sterile neutrino radiative decay. However, using the same data, Nieto & Mirabal (2010) claim that all lines in the X-ray spectrum can be explained by residual background emission and spurious features arising from an incorrect modelling of the latter. On the other hand, Boyarsky et al. (2010) analyse a combined sample of *XMM* observations of M31, Willman 1 and Fornax dSph as well as *Chandra* data for Sculptor dSph, finding no evidence of a spectral feature at 2.5 keV, and confirming the previous findings of Watson et al. (2006). [See, however, Kusenko & Loewenstein (2010) for a discussion of systematics.] Mirabal (2010) further used archival *Swift* XRT observation of the Milky Way satellite Segue 1, an ultrafaint dwarf galaxy with extreme mass-to-light ratio ($M/L >$

⋆E-mail: enrico.borriello@desy.de
†Visiting Associate, California Institute of Technology, Pasadena, CA 91125, USA.

1300; see Geha et al. 2009; Simon et al. 2011). They find no evidence of emission lines due to neutrino decay either and put upper limits on its parameter space.

In this work, we make use of archival *XMM–Newton* observations of the diffuse and unresolved components' emission of the inner disc of M33 (Owen & Warwick 2010). We set constraints on the sterile neutrino parameter space and compare them with analogous results previously found in the literature.

The paper is organized as follows. In Section 2, we summarize the data set used in our analysis and the results we get. In Section 3, we explore the consequences of our null detection in terms of bounds on the sterile neutrino parameter space. In Section 4, we set our conclusions.

2 X-RAY DATA ANALYSIS

The X-ray data used in this work are those already discussed extensively by Owen & Warwick (2010), and summarized here for completeness. The original observations were part of the Pietsch et al. (2004) survey of M33. Among the entire data set covering M33, we used only the observations #0102640101, #0102642301 and #0141980801 from the EPIC-PN detector, i.e. the same as used by Owen & Warwick (2010) for their spectral analysis (see their section 2.3) and covering the central part of the M33 disc out to a distance of ∼3.5 kpc, with observing times ranging from 7 to 10 ks. The details of the X-ray data reduction (temporal filtering, event screening, etc.) can be found in Owen & Warwick (2010). We wish to emphasize here that the data were spatially filtered in order to remove the contamination due to bright sources down to a luminosity of 2×10^{35} erg s^{-1}. A residual contamination is estimated by the authors which, as done in the referred paper, is taken into account in the following spectral analysis.

Appropriate auxiliary response files and response matrix files for the source-filtered region were created, while background files were produced from 'blank-sky' fields extracted from a region of sky close to M33, and 'filter-wheel closed' data to produce a background spectrum (again see details in Owen & Warwick 2010). The final spectra for the three observations are shown in Fig. 1.

We first verified that we were able to reproduce the Owen & Warwick (2010) results, fitting (using the Cash statistics) the data

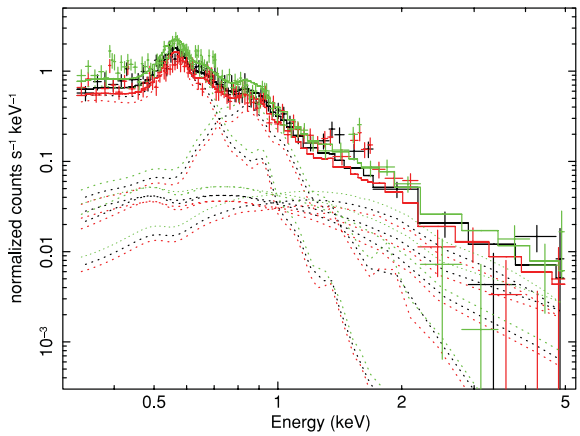

Figure 1. The X-ray spectrum of the M33 inner region, from the PN camera; the best-fitting model discussed in the text is overlaid, together with the individual components of the model. Note that only the two thermal components (those peaking at ∼0.6 and ∼0.9 keV) are free to vary, while all the others (due to the bright source contribution) are fixed to the residual flux expected to leak outside the masked region.

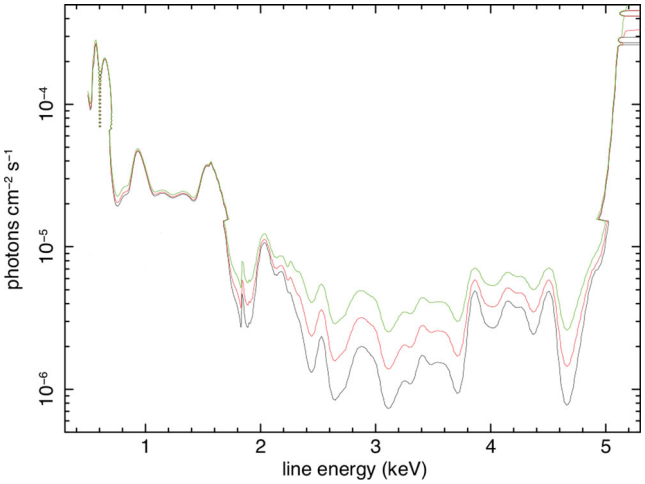

Figure 2. 68, 90 and 99 per cent limits (blue, red and green line, respectively) on the unresolved line normalization in the 0.5–5 keV energy interval.

with XSPEC 12.6 software[1] using a multicomponent model consisting of two thermal plasmas subject to Galactic absorption of $N_{\rm H} = 7.5 \times 10^{20}$ cm^{-2}, constrained to solar abundance, with temperatures of $kT = 0.2$ and 0.6 keV. We also tested the use of models with subsolar ($Z_\odot = 0.1$) metallicity but the results are consistent with those assuming solar metallicity. In addition, a power-law component was added to account for the 9 per cent flux from the bright sources leaking outside the masked regions; the bright ULX in the galaxy centre, which can be fitted with a more complex spectrum (power law, disc blackbody and intrinsic absorption), was treated separately, assuming that 3 per cent of its flux spills into our source-filtered region, as done in Owen & Warwick (2010). We then added an unresolved line to our spectral model, and fitted iteratively the whole spectrum in the range 0.5–5 keV allowing the line flux, and the thermal components' parameters (temperature and normalization), free to vary.

We computed the 68, 90 and 99 per cent confidence levels for two interesting parameters (line flux and central energy), shown in Fig. 2, sampling our energy range in steps of 20 eV, in order to fully exploit the EPIC spectral resolution. We note that several residual features are visible in the fitted spectrum, such as the emission lines around 1.5 keV due to the Al Kα line. Furthermore, the spectral model we use does not account for unresolved point sources below the 2×10^{35} erg s^{-1} threshold; this contribution is estimated by Owen & Warwick (2010) to be <1 per cent of the bright source emission. In order to minimize the uncertainties involved in refining the background spectrum, or in extrapolating the point source luminosity function to lower fluxes, we prefer to leave these contributions in the data, thus obtaining conservative lower limits on the DM line flux.

For consistency, as well as because of the very detailed checks performed in the Owen & Warwick (2010) work, we prefer to use here the original data. None the less, we checked the robustness of our results with respect to an update of the calibration software repeating the analysis – initially performed with SAS v8 – with the new SAS v11. The ratio between the flux upper limits derived with the old and new calibrations is plotted in Fig. 3, and shows that calibration issues introduce an uncertainty, at most, of a factor of 2 in the result. We reasonably expect that further releases of the calibration software will not change the result more than this.

[1] http://heasarc.nasa.gov/xanadu/xspec/

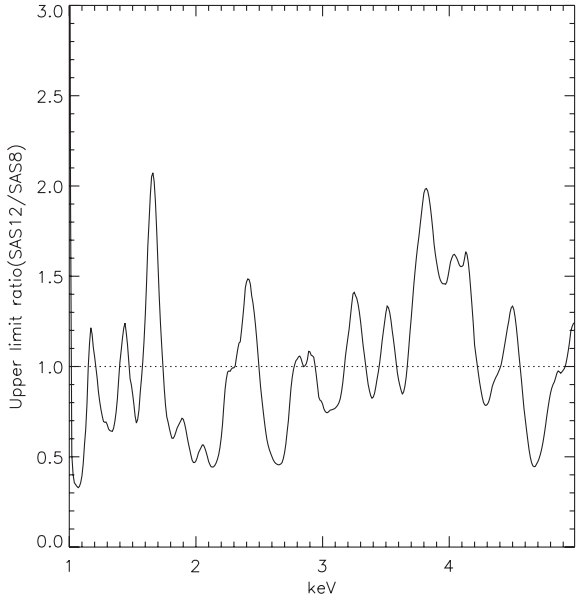

Figure 3. Ratio between the flux upper limits derived with the old (SAS v8) and new (SAS v11) calibrations. Calibration issues introduce at most a factor of 2 uncertainty in the result.

3 X-RAY FLUX FROM STERILE NEUTRINO DARK MATTER

We use the upper limits on the X-ray line flux derived in the previous section to constrain the possible contribution to M33 X-ray emission due to a radiative decay of sterile neutrino DM. This is done assuming that this additional contribution to the flux cannot exceed the upper limit deduced in the previous section.

Majorana sterile neutrinos may decay to a photon and an active neutrino (Pal & Wolfenstein 1982). The decay width of the process is[2]

$$\Gamma(\nu_s \rightarrow \gamma \nu_a) = 1.36 \times 10^{-32} \frac{\sin^2(2\theta)}{10^{-10}} \left(\frac{m_s}{\mathrm{keV}}\right)^5 \mathrm{s}^{-1},$$

where θ is the neutrino mixing angle and m_s – the double of the emitted photon energy – is the mass of the sterile neutrino.

The resulting flux at the Solar system position is $\Phi = \Gamma\, \Omega\, S/4\pi m_s$, in which Ω and S represent the angular size and the column density of the emitting region, respectively. In order to evaluate the DM column density, defined as the integral of the mass density along the line of sight, we need to parametrize the matter content of M33. Since there is no universal consensus on the DM halo profile in M33, we tried both the cored and spiked profiles that are consistent with the galaxy rotation curve (Corbelli 2003). The cored case is well represented by a Burkert density profile (Burkert 1995)

$$\rho(r) = \rho_0 (1 + x)^{-1} (1 + x^2)^{-1},$$

while the spiked profile is well described by an NFW density distribution (Navarro, Frenk & White 1997)

$$\rho(r) = \rho_0 x^{-1} (1 + x)^{-2},$$

with $x = r/r_0$. We consider two extremal cases among the various fits obtained in Corbelli (2003), taking the 3σ lower limit for the DM density in the Burkert case, and the 3σ upper one in the NFW case. This way we are taking into account the corresponding 3σ variation of the M/L in the inner part of M33 (Corbelli 2003). Their defining parameters are given in Table 1. Profiles with a central slope steeper than r^{-1} like the Moore profile (Moore et al. 1999) are instead excluded (Corbelli 2003).

[2] For Dirac sterile neutrinos, the decay width is half the one assumed here (Pal & Wolfenstein 1982).

Table 1. DM profile parameters.

Model	r_0 (kpc)	ρ_0 (GeV c^{-2} cm^{-3})
NFW	35	0.0765
Burkert	12	0.336

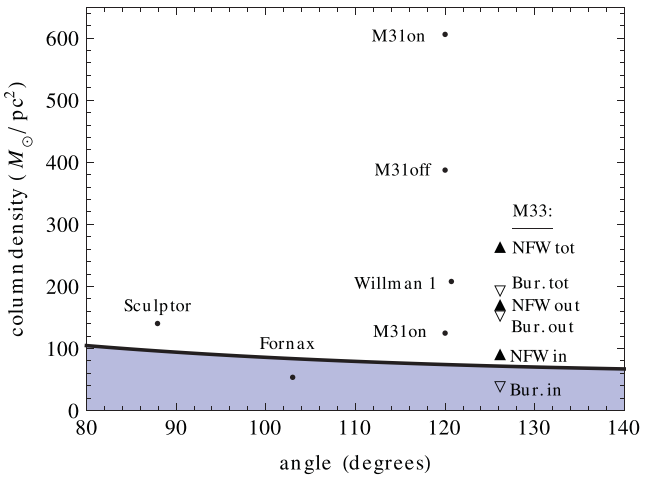

Figure 4. Column density for both mass parametrizations of M33 considered here compared to the ones assumed in previous similar analysis. The angle gives the angular distance from the galactic centre (126.°1 in the case of M33). The solid line represents the column density of the Milky Way (see text for more details).

Fig. 4 shows the DM column density for the various parametrizations of M33 considered here: filled triangles in the NFW case, empty triangles for a Burkert profile. We assumed an infinite halo in calculating the mean surface density, because we checked that repeating the calculation for a 17 kpc radius halo (the minimum possible radius, corresponding to the furthest observation in Corbelli 2003) will change the result by a factor of $\sim$1.3. In each case, we considered separately the inner region (in) of the galaxy – corresponding to the central 3.5 kpc bulge – and the outer part (out) of it – defined as the cylindrical volume corresponding to the same angular region and from which the central bulge has been subtracted. In addition, we also considered the sum of both contributions (tot). In all the cases, we took into account only the flux coming from the elliptical region analysed in Owen & Warwick (2010). The values we obtain for the column density range from 40.4 to 266 $\mathrm{M}_\odot\,\mathrm{pc}^{-2}$. This precaution addresses the concerns raised by Kusenko & Loewenstein (2010) about the uncertainties affecting the DM profile in the central region of the galaxy (see next section). A comparison is made with the column density of the Milky Way and the other systems considered in Loewenstein & Kusenko (2010) and Boyarsky et al. (2010). In evaluating the total flux at the Solar system position, we added up the contribution due to the Milky Way along the M33 line of sight, evaluated according to the DM density parametrization given in Strigari et al. (2008).

Fig. 5 shows the regions of the parameter space ($\sin^2 2\theta$, m_s) excluded by the X-ray observations of M33. The main assumption

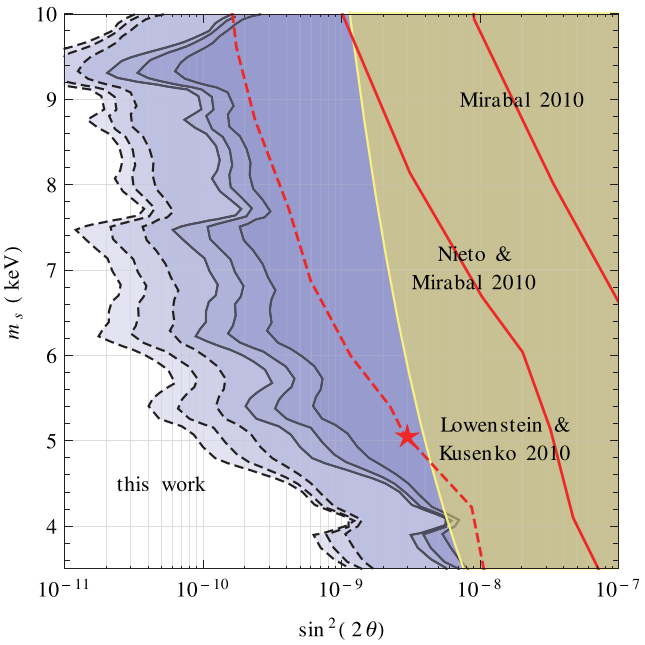

Figure 5. Sterile neutrino parameter space. The light blue regions are excluded by X-ray observations of M33 (limits at 68, 90 and 99 per cent). The least (Bur. in, solid line) and the most (NFW tot, dotted line) stringent bounds are represented. The red thick solid lines represent the constraints on sterile neutrinos derived for Segue 1 (Mirabal 2010) and Willman 1 (Nieto & Mirabal 2010). The red thin dashed line corresponds to the upper bound in Willman 1 (Loewenstein & Kusenko 2010). The star represents the model of Loewenstein & Kusenko (2010). The yellow line gives the models in which the cosmological amount of DM is entirely made up by sterile neutrinos. The yellow region is excluded by overclosure. The exclusion regions are deduced assuming 100 per cent of DM is made up of sterile neutrinos.

here is that the DM halo is entirely made up by sterile neutrinos. Limits are shown at 1σ, 2σ and 3σ confidence levels. We show the most and the least stringent cases, among the six we considered here: NFW tot (dotted lines) and Bur. in (solid lines), respectively. The yellow line gives the models in which the cosmological amount of DM is entirely made up by sterile neutrinos. The yellow region is therefore excluded by overclosure. The star represents the model of Loewenstein & Kusenko (2010), which is found to be inconsistent with the observed X-ray emission from M33.

4 DISCUSSION AND CONCLUSIONS

Let us now summarize the assumptions under which our results were obtained and the uncertainty affecting them. As pointed out in Kusenko & Loewenstein (2010), the interaction of DM with baryons could have the effect of expelling the DM out of the central part of a spiral galaxy (Klypin, Zhao & Somerville 2001). DM could therefore provide only a subdominant contribution to the total amount of mass in the central part of M33. This is the reason why we separated the emission along the line of sight into two contributions, the one produced in the innermost region of M33 and the contribution coming from the two external cylinders. Interestingly (see Fig. 4), these external (out) contributions – whose mass distribution is determined on a more stable basis – are the ones giving the most stringent bounds. This makes our results stable against the main criticism raised by Kusenko & Loewenstein (2010). We stress that our results change by less than one order of magnitude because of the uncertainty affecting the DM density distribution, which could be either cored or spiked at the centre of M33.

An additional uncertainty factor is represented by the effect of photometric absorption. This will reduce the detected X-ray flux, thus resulting in an underestimate of the M33 DM emission. We note however that (i) galactic absorption has already been taken into account in the spectral fitting described in Section 2, (ii) photometric absorption is relevant only in the soft X-ray band below 2 keV, and thus the limits in the hard energy range are essentially unaffected, (iii) additional intrinsic M33 absorption may be present but likely with a low covering factor. The population of M33 X-ray sources for instance [see e.g. discussion in Foschini et al. (2004) and Grimm et al. (2007)] does not reveal widespread absorption, and anyway with $n_{\rm H}$ less than a few $\times 10^{21}$ cm^{-2} which results in a factor of $\sim$2 reduced flux at 1 keV. Nevertheless, to evaluate the effect that absorption might have on our estimates, we could simply divide by $\sim$2 the emission coming from the back cylinder. This would result in a 25 per cent reduction of the total flux (out cases), which does not affect our main results. We also need to point out that in our analysis we did not try to fine tune the background removal, nor did we model the contribution of the unresolved X-ray binary population, in order to avoid biases due to the poor knowledge of these contributions to the overall X-ray emission. This choice results in conservative upper limits on the M33 DM content, since the estimated emission is actually overestimated.

In summary, we make use of archival *XMM–Newton* observations of the diffuse and unresolved components' emission of the inner disc of M33 (Owen & Warwick 2010), finding no evidence for line emission compatible with sterile neutrino radiative decay. We accordingly set bounds on sterile neutrino parameter space under the assumption that they account for the entire DM content of M33. In particular, we have found no evidence for the emission by 5 keV neutrinos deduced by Loewenstein & Kusenko (2010).

ACKNOWLEDGMENTS

EB acknowledges financial support by the Deutsche Forschungsgemeinschaft through SFB 676 'Particles, Strings and the Early Universe: The Structure of Matter and Space-Time'. EB and GM acknowledge support by the INFN I.S. FA51 and the PRIN 2008 'Fisica Astroparticellare: Neutrini ed Universo Primordiale' of the MIUR. MP acknowledges support from PRIN 2009 of the MIUR. GL thanks the California Institute of Technology for hospitality.

REFERENCES

Biermann P. L., Kusenko A., 2006, Phys. Rev. Lett., 96, 091301
Boyarsky A., Ruchayskiy O., Iakubovskyi D., Walker M. G., Riemer-Sorensen S., Hansen S. H., 2010, MNRAS, 407, 1188
Burkert A., 1995, ApJ, 447, L25
Corbelli E., 2003, MNRAS, 342, 199
Dodelson S., Widrow L. M., 1994, Phys. Rev. Lett., 72, 17
Feng J. L., 2010, ARA&A, 48, 495
Foschini L., Rodriguez J., Fuchs Y., Ho L. C., Dadina M., Di Cocco G., Courvoisier T. J.-L., Malaguti G., 2004, A&A, 416, 529
Geha M., Willman B., Simon J. D., Strigari L. E., Kirby E. N., Law D. R., Strader J., 2009, ApJ, 692, 1464
Grimm H.-J., McDowell J., Zezas A., Kim D.-W., Fabbiano G., 2007, ApJS, 173, 70
Klypin A., Zhao H., Somerville R. S., 2002, ApJ, 573, 597
Komatsu E. et al., 2011, ApJS, 192, 18
Kusenko A., 2009, Phys. Rep., 481, 1
Kusenko A., Loewenstein M., arXiv:1001.4055

Loewenstein M., Kusenko A., 2010, ApJ, 714, 652
Loewenstein M., Kusenko A., Biermann P. L., 2009, ApJ, 700, 426
Mirabal N., 2010, MNRAS, 409, L128
Moore B., Ghigna S., Governato F., Lake G., Quinn T. R., Stadel J., Tozzi P., 1999, ApJ, 524, L19
Navarro J. F., Frenk C. S., White S. D. M., 1997, ApJ, 490, 493
Nieto D., Mirabal N., 2010, arXiv:1003.3745v3
Owen R. A., Warwick R. S., 2010, MNRAS, 403, 558
Pal P. B., Wolfenstein L., 1982, Phys. Rev. D, 25, 766
Pietsch W., Misanovic Z., Haberl F., Hatzidimitriou D., Ehle M., Trinchieri G., 2004, A&A, 426, 11
Porter T. A., Johnson R. P., Graham P. W., 2011, ARA&A, 49, 155
Simon J. D. et al., 2011, ApJ, 733, 46
Strigari L. E., Koushiappas S. M., Bullock J. S., Kaplinghat M., Simon J. D., Geha M., Willman B. M., Willman B., 2008, ApJ, 678, 614
Watson C. R., Beacom J. F., Yuksel H., Walker T. P., 2006, Phys. Rev. D, 74, 033009

This paper has been typeset from a TEX/LATEX file prepared by the author.